Automatic Extraction of Training Sets Using AIS in CNN for Ship Detection from SAR Image

Juyoung Song (1), Duk-jin Kim (1), Ki-mook Kang (1)

[1] Seoul National Univ., 1 Gwanak-ro, Gwanak-gu, Seoul, 08826, Korea
Email: 96daniel@snu.ac.kr; djkim@snu.ac.kr; mook0416@snu.ac.kr;

KEY WORDS: Vessel, Deep learning, Bounding box, Azimuth offset

ABSTRACT: Ship detection from SAR images plays a crucial role in monitoring maritime safety and securing marine resources. Among variety of ways in detecting ships, convolution neural network (CNN) is widely applied as a deep learning method to efficiently sort out vessels using their scattering characteristics. Obtaining training set data has been an important issue since it is a factor that may influence the entire procedure and result of CNN. Retrieval of training set data for object detection including ship however, has been often conducted manually.
This research presented an automatic extraction of training set data applying automated identification system (AIS) which was mainly used as a way of evaluation of ship detectors. Since AIS provides not only spatial location of ships but also their velocity, heading azimuth and receiver's location inside the ship, it makes possible calculate the precise location of the ship. Azimuth offset, migration of an object in SAR image caused by Doppler shift, was taken into account in addition. Training set information of spatial location that has undergone the proposed automatic extraction method was applied to SAR images taken in the vicinity of southeastern coastlines of Korea, from TanDEM-X, as a validation. Usage of AIS in retrieving training set presented a possibility of automatic extraction of vessels in low resolution SAR images.

1. INTRODUCTION

Continuous monitoring of vessels in vicinity of coastal area is an essential factor in maritime safety issues (Rowlands et al., 2019). Handful of remote sensing machinery has been applied, including electro-optical, infrared, hyperspectral sensors, SAR etc. Among these tools, SAR image acts as an indispensable tool in cruise monitoring, backed by independence from weather conditions and deprivation of sunlight. Currently, research of machine learning within SAR image has been widely conducted as an effective tool of detecting and classifying ships automatically.
For deep learning procedure which mainly seeks to improve accuracy and efficiency, selection of training set data is a top priority since deep learning network is constructed based on training set data (Shin et al., 2016). Manual extraction of training set data has hitherto been a widely used method in obtaining those (Shao et al., 2018). This method however is often conducted by naked eye and can be questioned since scattering character of radar may not be fully recognized. In case of vessels, automated identification system (AIS) provides credible information on ships' location and widely fused with SAR images as verification.
Attempt of fusing AIS with SAR images has been continuously implemented. Combining TanDEM-X image with AIS and satellite AIS (SatAIS), which allows to offer a worldwide ship monitoring system based on spaceborne system, was used for testing ship detection in stripmap mode (Brusch et al., 2011). Feature contrast between AIS information and SAR image was presented and testified by support vector machine (SVM) and its variations (Lang et al., 2018). In addition, AIS was also applied in verifying ship classification method using polarimetric character of SAR (Pelich et al., 2019), or integrated with multispectral images (Kurekin et al., 2019).
This research suggests a novel application of AIS-SAR fusion; directly retrieving training set data from AIS and SAR image rather a conventional way of verifier (Snapir et al., 2019). Given that AIS data provides credible location of vessels, it is possible to use AIS for extracting training set by applying it on SAR images. Since location of AIS sensor inside the ship can be figured out by using the vessels' character, training set could be extracted considering course-over-ground (COG) and speed-over-ground (SOG) of the ship. However, line-of-sight (LOS) velocity of moving object inside SAR image causes azimuth offset, parallel migration of scatterer to azimuth. Correction of azimuth offset was also calculated using incidence angle and slant range between satellite and scatterers. Offset-corrected position of vessel was finally presented as training set in coordinate form of bounding box, frequently used form of training set data in object detection.

2. DATA ACQUISITION

SAR images taken from TanDEM-X satellite were used as image dataset, in vicinity of Korea Strait. Since Korea Strait is adjacent to Busan, the largest harbor in South Korea, and a critical passage connecting East Sea and East China Sea, monitoring on this region is expected as a valuable example of marine surveillance.

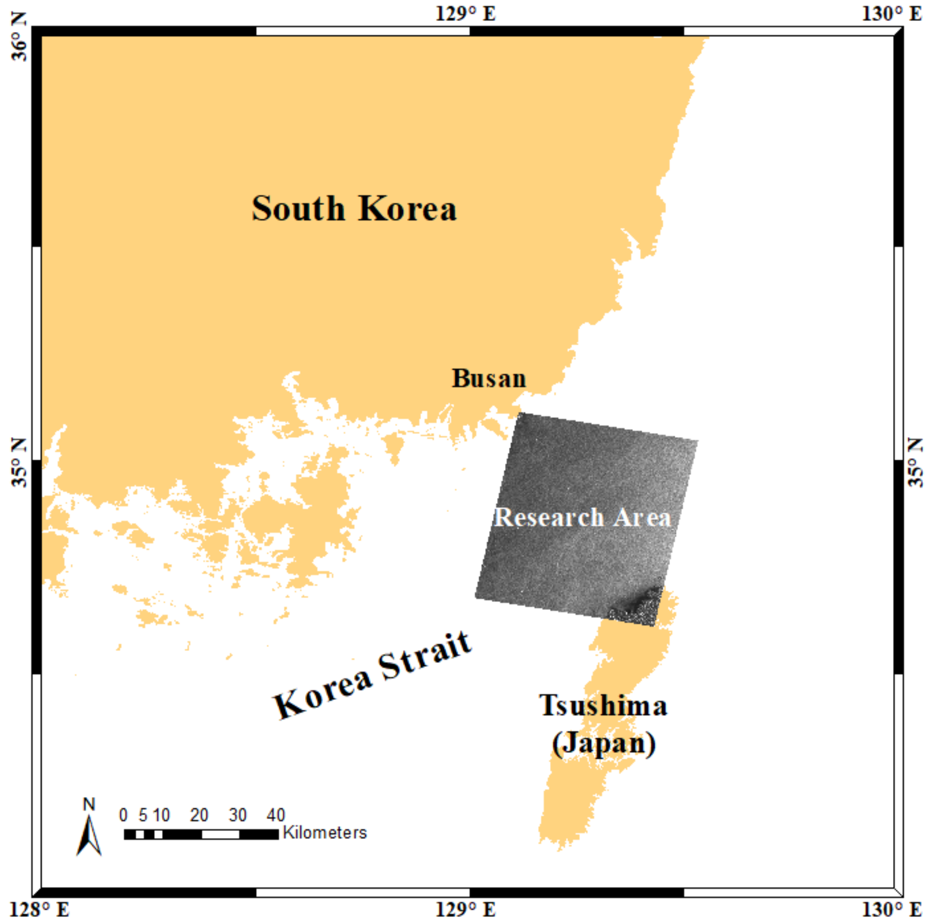

Figure 1. Spatial location of research area in detail. 8 TanDEM-X images used in research cover Korea Strait, between South Korea and Japanese Tsushima Island.

AIS data was provided on behalf of the research by Ministry of Oceans and Fisheries of Korea (MOF). The data includes discrete position of vessel in latitude and longitude, ID, name, COG and SOG of each vessel. MOF also provides position of AIS sensor inside the vessel, which can be matched with AIS data using each vessel's ID. Position of AIS sensor inside vessel is given as a form of 4 direction coordinates: DimA, DimB, DimC and DimD.

3. METHODOLOGY

3.1 Position Estimation Using Azimuth Offset Calculation

Using discrete positions of each ship, the expected positions of vessels at the time of satellite photography were linearly interpolated using averaged time between initiation and termination of each SAR image's acquisition time. Not only spatial position, longitude and latitude, but also COG and SOG of each vessel underwent linear interpolation. However, scatterer in SAR image which contains LOS velocity inevitably involves azimuth offset, where object is shifted parallel to satellite azimuth direction as described in equation 1.

$$A_{offset} = \frac{V_{obj} * R_{slant} * cos\theta_i}{V_{sat}} \quad \text{(Eq. 1)}$$

According to equation 1, azimuth offset A_{offset} is a function of 4 variables V_{obj}, V_{sat}, R_{slant}, θ_i, which stands for LOS velocity of moving scatterer, satellite velocity, slant range between satellite and moving scatterer, incidence angle respectively. In case of this research where image from TanDEM-X is applied, $V_{sat} = 7600\mathrm{m/s}$ is used. Also, LOS velocity of each vessel was measured using equation 2, where θ_{head} stands for heading angle of satellite in radian. Interpolated SOG and COG of each vessel were given as an input variable in equation 2.

$$V_{obj} = SOG * \cos(\frac{\pi}{2} + \theta_{head} - COG) \quad \text{(Eq.2)}$$

For exact calculation of R_{slant} and θ_i of every position of vessel, satellite state vector was implemented. Each TanDEM-X image file offers position of satellite in geocentric coordinates. When combined with geocentric coordinate grid indicating the target area, accurate field of R_{slant} and θ_i can be obtained. Implementing geocentric location of satellites, it is possible to define the accurate position of satellite on each azimuth line. This can be accomplished by deriving elliptic path of TanDEM-X, which can be described by using 6 Kepler orbital parameters of path: eccentricity, semi-major axis, inclination, longitude of ascending node, argument of periapsis and true anomaly. As 6 Kepler orbital parameters define a single elliptic satellite orbit, averaged parameters creates single satellite orbit which is nearly identical to true elliptic path of TanDEM-X. After field of R_{slant} and θ_i between AIS sensor and satellite are retrieved, A_{offset} of each vessel was calculated using equation 1 and applied on SAR images.

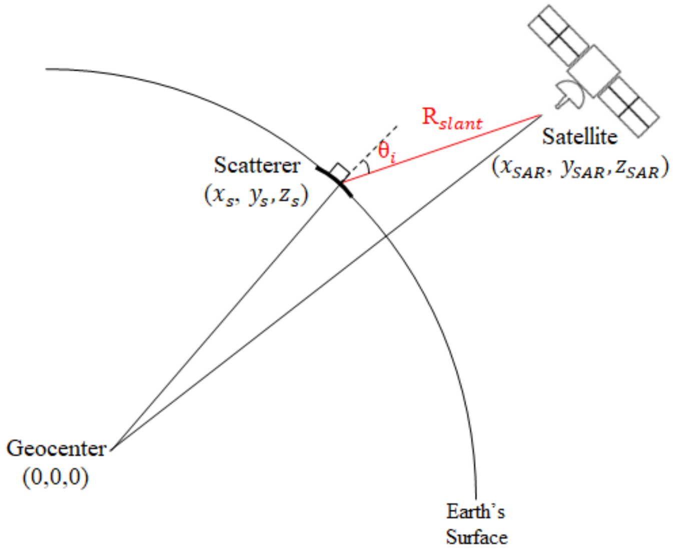

Figure 2. Relative position of scatterer and satellite. R_{slant} can be calculated using distance between 2 geocentric coordinates of SAR satellite and scatterer. θ_i is derived by applying cosine law on triangle connecting geocenter-scatterer-satellite.

3.2 Extraction of Training Set Data for Object Detection

Once the accurate position of vessel was defined, successive procedure of extracting the training set bounding box in form of (x, y, w, h) follows. For this procedure, position of AIS sensor inside vessel in meters in AIS data is used. 4 dimensions explaining absolute position of AIS in vessel in meters are described in figure 3.

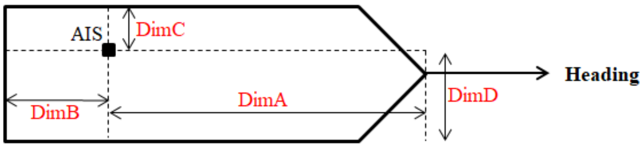

Figure 3. AIS position inside ship and dimensions explaining it: DimA, DimB, DimC and DimD.

With COG, SOG and 4 dimensions of AIS position, bounding box of vessel can be accurately calculated. COG indicates the heading angle of vessel with respect to North Pole, and SOG stands for velocity of vessel in COG direction. The top left corner's coordinate (x, y), width and height of the rectangular bounding box (w, h) were calculated, without deliberating rotation angle of bounding box.

In 4 different cases depending on COG, where $0 \leq \mathrm{COG} < \frac{\pi}{2}$, $\frac{\pi}{2} \leq \mathrm{COG} < \pi$, $\pi \leq \mathrm{COG} < \frac{3\pi}{2}$ and $\frac{3\pi}{2} \leq \mathrm{COG} < 2\pi$, (x, y, w, h) coordinates were calculated. Using 4 dimensions of AIS inside vessel and rotation angle expressed as COG in AIS, anomaly distance between AIS location and coordinate point (x, y), width and height is denoted as a function of 4 dimensions and COG.

4. RESULTS AND DISCUSSION

Applying proposed methods on given AIS data, coordinates from each SAR images were successfully extracted as table 2. In 9 TanDEM-X images, total 142 training set data of vessels were effectively retrieved. 2 examples of extracted training set are shown in figure 4; along with data before azimuth offset correction.

Table 1. SAR satellite image data profile and number of extracted vessel for training set in each image

Satellite	Date of Acquisition(UTC)	Time of Acquisition(UTC)	Center Latitude (˚N)	Center Longitude(˚N)	Center Incidence Angle(˚)	Heading (˚)	Center Range Slant(m)	Training set extracted
TanDEM-X	13-02-2012	21:35:46~21:35:53	34.8626	129.2887	21.2639	191.1972	547501.50	23
TanDEM-X	06-03-2012	21:35:46~21:35:53	34.8624	129.2917	21.2348	191.1975	547497.86	16
TanDEM-X	28-03-2012	21:35:47~21:35:54	34.8604	129.2895	21.2542	191.1977	547497.86	21
TanDEM-X	06-12-2012	21:35:53~21:36:00	34.8671	129.2905	21.2519	191.2024	547404.19	17
TanDEM-X	17-12-2012	21:35:52~21:35:59	34.8637	129.2914	21.2489	191.2020	547393.28	18
TanDEM-X	28-12-2012	21:35:52~21:35:59	34.8670	129.2886	21.2550	191.1999	547393.28	10
TanDEM-X	08-01-2013	21:35:52~21:35:59	34.8655	129.2875	21.2709	191.1999	547389.64	17
TanDEM-X	19-01-2013	21:35:51~21:35:58	34.8653	129.2877	21.2911	191.1995	547381.45	20

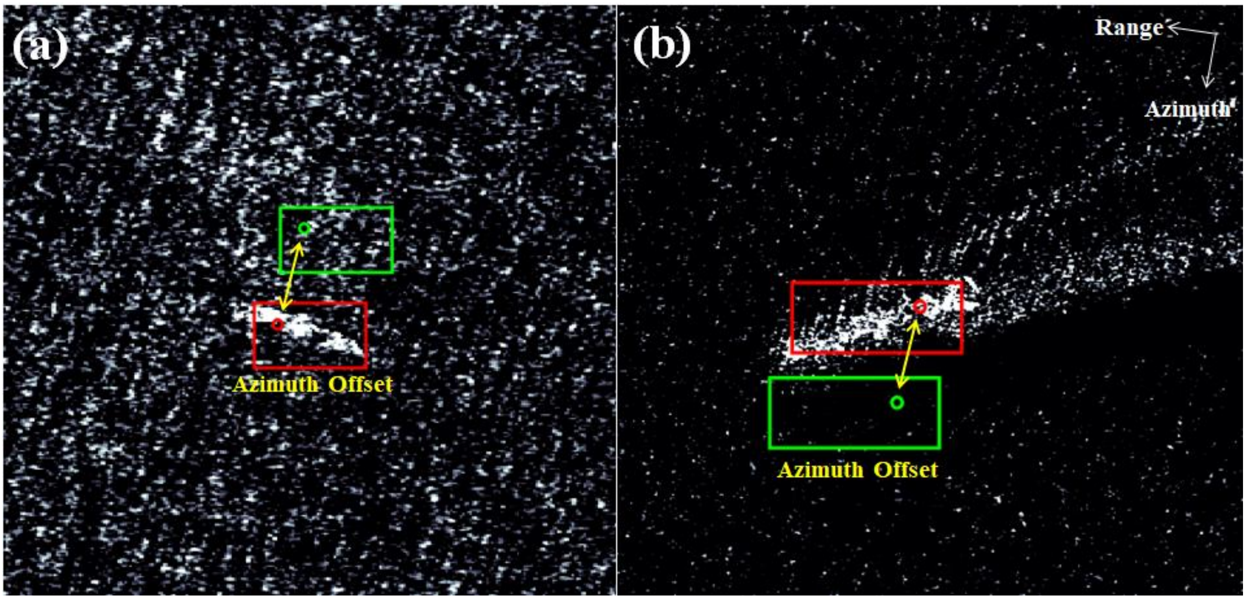

Figure 4. Training set bounding boxes and AIS positions of 2 vessels on TanDEM-X image acquired on (a) February 13th, 2012 and (b) March 28th, 2012. Green rectangles and circles indicate extracted training set data and AIS position before azimuth offset correction, where red rectangles and circles denote extracted training set data and AIS position after azimuth offset correction. Yellow lines denote azimuth offset.

Due to vessels that operate without AIS sensors, not all vessels can be detected and their training set data can be extracted by implementing proposed method. These vessels may be detected using neural network model which applies training set data of vessels with their AIS sensors turned on. In addition, current linear interpolation method assumes the time of interpolation as averaged time of 2 acquisition times. This procedure can be corrected when interpolation time is applied differently depending on each azimuth line.

5. CONCLUSION

This research opened a new possibility of extracting training set of vessels from SAR image by suggesting a novel method of bounding box extraction and applying it to 8 TanDEM-X images. Instead of previous manual extraction of training set data, often deprived of precision, verified AIS data were directly applied. Retrieved training set were in style of coordinate, (x, y, w, h), enabling it for direct implementation on CNN.

ACKNOWLEDGEMENTS

This work was supported by Ministry of Oceans and Fisheries (no. 20180455, Technological Development for Practical Applications of Multi-Satellite Data to Maritime Issues) and Korea Hydrographic and Oceanographic Agency (KHOA) through the application program of Ieodo Ocean Research Station.

REFERENCES

Rowlands G., Brown J., Soule B., Boluda P. T. and Rogers A. D. 2019. Satellite Surveillance of Fishing Vessel Activity in the Ascension Island Exclusive Economic Zone and Marine Protected Area. Marine Policy, 101, pp. 39-50.

Shin H.-C., Roth H. R., Gao M., Lu L., Xu Z., Nogues I., Yao J., Mollura D. and Summers R. M. 2016. Deep Convolutional Neural Networks for Computer-Aided Detection: CNN Architectures, Dataset Characteristics and Transfer Learning. IEEE Transactions on Medical Imaging, 35 (5), pp. 1285-1298.

Shao Z., Wu W., Wang Z., Du W. and Li C. 2018. SeaShips: A Large-Scale Precisely Annotated Dataset for Ship Detection. IEEE Transactions on Multimedia, 20 (10), pp. 2593-2604.

Brusch, S., Susanne L., Fritz T. and Soccorsi M. 2011. Ship Surveillance with TerraSAR-X. IEEE Transactions on Geoscience and Remote Sensing, 49 (3), pp. 1092-1102.

Lang, H., Wu S. and Yongjie X. 2018. Ship Classification in SAR Images Improved by AIS Knowledge Transfer. IEEE Transactions on Geoscience and Remote Sensing, 15 (3), pp. 439-443.

Pelich, R., Chini M., Hostache R., Matgen P., Lopez-Martinez C., Nuevo M., Ries P. and Eiden G. 2019. Large-Scale Automatic Vessel Monitoring Based on Dual-Polarization Sentinel-1 and AIS Data. Remote Sensing, 11 (9), pp. 1078.

Kurekin, A. A., Loveday B. R., Oliver C., Quartly G. D., Miller P. I., Wiafe G. and Agyekum K. A. 2019.Operational Monitoring of Illegal Fishing in Ghana through Exploitation of Satellite Earth Observation and AIS Data. Remote Sensing, 11 (3), pp. 293.

Snapir B., Waine T. W. and Biermann L. 2019.Maritimee Vessel Classification to Monitor Fisheries with SAR: Demonstration in the North Sea. Remote Sensing, 11 (3), pp. 353.